CSCE Annual Conference

Growing with youth – Croître avec les jeunes

Laval (Greater Montreal)

June 12 - 15, 2019

SEVERE CORROSION BEHAVIOR OF TWO-WAY SLABS UNDER DIFFERENT ACCELERATED CORROSION TECHNIQUES

Said, Mahmoud. E[1,3], Hussein, Amgad[1], and Gillis, Nick.[2]

[1] Civil Engineering Department, Memorial University, Canada
[2] SNC Lavalin Inc, Canada
[3] meaeaas2@mun.ca

Abstract: The behaviour of severe corrosion was illustrated in this paper using two different accelerated techniques. Each accelerated technique reached the same corrosion level, 50% mass loss. One technique used constant voltage and the other one used constant current. Two full-scale two-way slabs of dimensions 1900 mm × 1900 mm × 150 mm were cast for this purpose. A column stub with a cross-sectional area of 250 mm × 250 mm and a height of 200 mm was attached to each slab. The corrosion behaviour for each slab was assessed based on the results of the current, half-cell potential, corrosion cracks pattern, and mass loss. Both techniques showed a close agreement between the actual and the theoretical mass loss, which was calculated using Faraday's equation. It was observed that the corrosion cracks in constant voltage technique were induced randomly while in the other slab induced above the corroded bar. This could be attributed to the current value that was kept constant in constant current technique, while the current value varied in the constant voltage technique and reached high values. This could increase the probability of a constant voltage technique to cause more damage than a constant current.

Keywords: Severe corrosion, Constant voltage, Constant current, Two-way slabs

1 Introduction

Corrosion is an electrochemical process that occurs due to a difference in the electrical potential along the reinforcement. Concrete and metal elements need a long period to corrode, which make studying corrosion of those elements very hard. Therefore, researchers innovated some techniques to accelerate the corrosion process. These techniques save time and money, and help researchers to do more studies on the behavior of corroded elements. The researchers correlate between the accelerated corroded laboratory results and the real corrosion that occurs to existing structures (Davis, 2000). These techniques based on creating and accelerating an electrochemical potential between the embedded reinforcement (anode) inside concrete and an external or internal cathode in the presence of an electrolyte solution (El-Maaddawy and Soudki, 2003). Based on Faraday's equation, the current is a parameter on predicting the mass loss of corroded element. Therefore, Current is used to accelerating the corrosion process (Toongoenthong and Maekawa, 2004). Some researchers applied the current through the application of a constant voltage that was ranged from 5V to 30V (Amleh, 2000; Lee *et al.*, 2000; Ahwazi, 2001; Yoon *et al.*, 2001; Kumar *et al.*, 2012; Xia, Jin and Li, 2012; Deb and Pradhan, 2013; Pellegrini-Cervantes *et al.*, 2013; Al-Swaidani and Aliyan, 2015). Others applied the current through the application of a constant current that was ranged from $45\mu A/cm^2$ as a minimum value to $10400\mu A/cm^2$ as a maximum value (Almusallam *et al.*, 1996; Bonacci *et al.*, 1998; El-Maaddawy and Soudki, 2003; El-Maaddawy, Soudki and Topper, 2005; Kashani, Crewe and Alexander, 2013; Pritzl, Tabatabai and Ghorbanpoor, 2014; Talakokula, Bhalla and Gupta, 2014; Altoubat, Maalej and Shaikh, 2016). El Maaddawy & Soudki (2003)

recommended not to exceed the current density above 200μA/cm^2 because exceeding this value could cause a significant increase in crack width and strain response due to the corrosion. The authors also recommended avoiding using different current densities to reach different corrosion levels because this could misguide the analysis of the test results.

Altoubat et al. (2016) conducted a comparison study between the constant voltage and constant current techniques. They applied the corrosion on small-scale columns. The authors recommended constant current technique to be used as an accelerated method because the corrosion levels reached in a reasonable time comparing with constant voltage. However, constant current created damage in the specimen more than that by constant voltage.

Accelerated corrosion tests had been conducted on structural elements such as beams and one-way slabs. To the best of the authors' knowledge, there is only one study that has been carried out a comparison between the constant voltage and constant current techniques by applying them on two-way slabs. They reached a high level of corrosion 25% mass loss (Said and Hussein, 2019). Said & Hussein (2019) recommended using the constant current technique because of its time feasibility and the setup cost effectivity. Said & Hussein (2019) showed the challenges that could face researchers to induce corrosion in two-way slabs. Two-way slabs have a high density of bars compared to beams. Therefore, two-way slabs tests require data acquisition system with more channels to record the current during the corrosion process. Also, most data acquisition systems are more equipped to record voltage output rather than current. The availability of an acquisition system with a large number of channels in any laboratory could be a challenge. The lab-space availability is another important challenge; especially, the time period could reach several months to achieve the targeted corrosion level. The flexural reinforcement for two-way slabs consists of two layer; an upper and lower ones. In order to induce uniform corrosion in the targeted area, the connection points between bars should eliminate any electrical conductivity between them. Also, the compression mesh has to be isolated from the flexural one.

This paper aims to demonstrate a full comparison between accelerated corrosion techniques to reach severe corrosion levels, 50% mass loss, on two-way reinforced concrete slabs.

2 Experimental Program

2.1 Details of Test Specimens

Two identical slabs were under investigation on this study. The dimension of each slab is 1900 × 1900 × 150 mm. The reinforcement ratio is 1% distributed uniformly using 15M bars that are spaced at 190 mm. The concrete cover equals 30 mm. Figure 1 shows the details of a typical slab. Each bar was weighted and marked before casting the slab to use these values in calculating the actual mass loss at the end of the test. The intersection point of the flexural mesh was isolated using electrical tape to control and ensure uniform corrosion in each corroded bar. Each bar was connected by wires from each both sides to use it in the accelerated corrosion process. Each slab corroded to 50% mass loss. One slab corroded using constant voltage accelerated technique and labelled as SV. The other slab used constant current accelerated technique and labelled as SC.

2.2 Material Properties

The slabs cast based on the concrete mixture showed in Table 1. The concrete composition was designed to consider the exposure effect of de-icing salt on concrete horizontal elements based on the recommendation of ACI 318-14. This kind of exposure is classified as class F where the water to cement (w/c) ratio has not to exceeded 0.4 and the targeted strength has not be lowest than 40 MPa (ACI 318-14, 2014). The concrete was delivered from a local batch plant. Concrete cylinders

and prisms were poured to determine the compressive strength ($f_c^{'}$) and the modulus of rupture (f_r). The actual properties of the concrete and the reinforcement was shown in Table 2.

Table 1 Mixture Composition of Concrete Mix

Cement (kg)	w/c ratio	Coarse/fine ratio	Coarse aggregate (kg)	Fine aggregate (kg)	Maximum aggregate size (mm)	Fresh density (kg/m3)
350	0.4	1.3	1083	833	10	2407

Table 2 Steel and Concrete Properties

	Steel properties			Concrete Properties	
Designation	Area mm^2	f_y MPa	ε_y ($\mu\varepsilon$)	$f_c^{'}$ MPa	f_r MPa
15M	200	475	2200	41.1	3.82

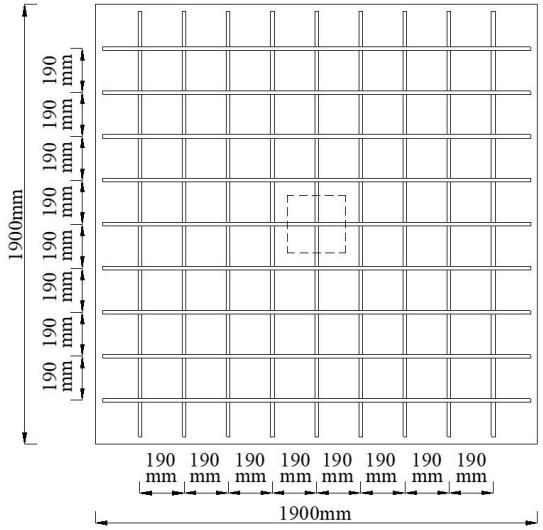

a. Flexural mat reinforcement 15M @ 190 mm

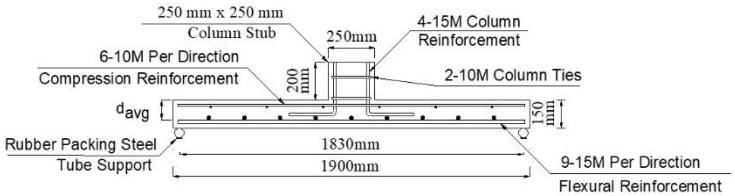

b. Cross-section of the slab

Figure 1: Details of a typical slab

2.3 Accelerated Corrosion Setup

The preparation of the accelerated corrosion setup started directly after pouring the concrete. First, the slabs were upside down in a levelled position then a dike was constructed above each slab around the targeted corroded area using foam sheets. A steel mesh was placed inside the dike to work as a cathode, where it was connected to the negative charge of the source of electricity. The tank was filled with an electrolyte solution (5% of chloride salt solution). The steel bar embedded inside the concrete was worked as an anode by connecting it with a source of a direct current. The theoretical mass loss is calculated based on Faraday's equation as shown in Eq. (1):

$$\text{Mass loss} = \frac{t\ i\ M}{z\ F} \quad (1)$$

Where t is the time passed in seconds, i is the current passed in amperes, M is atomic weight (for iron $M = 55.847$ g/mol), z is the ion charge (two moles of electrons) and F is Faraday's constant which is the amount of electrical charge in one mole of electron ($F = 96,487$) (Lachemi *et al.*, 2014).

2.3.1 Constant Voltage Technique Setup

Slab SV was set up through the application of a constant voltage technique. This technique required one power supply, data acquisition systems, current transducers, distribution board, electrolyte solution, steel mesh, and computer to process the data. The power supply was adjusted on a constant voltage of 15V and the output current was needed to be recorded. The most available data acquisition system in labs reads voltage only because the most output signal of the structural lab equipment represents on voltage. It is too expensive to buy a new data acquisition system to process current readings; especially the slab needs enough free channels to record the current for each corroded bar. Therefore, calibrated current transducers were used to convert the current reading to a voltage reading to record the data using the available data acquisition system in the lab. Each bar needs a separate source of current; therefore, a distribution board was used to distribute the positive terminal from the power supply to several outlet terminals with different current values but keeping the voltage constant at 15 V. This distribution board was constructed based on a parallel circuit mechanism, in which maintaining the voltage constant. The negative terminal was connected directly to the steel mesh that was immersed inside the electrolyte solution inside the dike.

2.3.2 Constant Current Technique Setup

Slab SC was set up through the application of a constant current technique. This technique required power supplies, electrolyte solution, and steel mesh. The number of power supplies is the same as the required number of corroded bars. Each bar is connected to a separate power supply that adjusted to a constant current value. This current value has not to exceed $200\mu A/cm^2$ to avoid any significant increase in crack width and strain response due to the corrosion as recommended by El-Maaddawy and Soudki, (2003). The corrosion time was starting to be counted when the half-cell potential read more than -350 mV to ensure that the occurrence possibility of corrosion was more than 90% (ASTM C876, 2015).

3 EXPERIMENTAL RESULTS AND ANALYSIS

3.1 Time-dependent corrosion tests results

3.1.1 Current Results

The constant current technique was used to corrode Slab SC by applying $200\mu A/cm^2$ that was equivalent to 0.15 A, where the length of corroded bar was 1480 mm. This current was applied for

290 days until reaching the targeted corrosion level of 50% mass loss. Constant current technique distinguish with its ability to determine the exact time requires to reach the targeted level of corrosion (Said and Hussein, 2019). The other slab SV was corroded by applying current with a constant voltage of 15 V. The current was monitored during the test using data acquisition system for each bar. Figure 2 shows the relation between the current and the elapsed time. The first point on the curve is an indication for the presence of the passivation layer around the rebar that prevent corrosion occurrence. The decreasing of the slope is an indication of the dissipation of the passivation layer. Once the slope became constant or gradually increased that consider as an indication of increasing the rate of corrosion (Cornet, Ishikawa and Bresler, 1968). After 69 days, the current had a sudden increase in the slope. The current value exceeded the initial current value. After 104 days there was a sudden decrease in the slope that followed by a constant rate of corrosion. After 202 days, the current had another jump that exceeded the first jump then the current dropped down until reaching the targeted corrosion level 50%. This behavior is different than what was reported by Said & Hussein (2019), regarding corroding a slab to 25% mass loss. This difference could return to reaching 50% mass loss, which considers more deeply study than the other one. Said & Hussein (2019) reported that after 25% mass loss, the current could reach high values which could increase the rate of corrosion. While in this study, it has been noticed two drops in the current, which mean that the current would not rise to an infinite value. These drops in the current could be attributed to the presence of corrosion products that could act as a barrier in cracks openings for current to reach the bars. The jumping of current again could be attributed that the cracks become wider which give more access to the current to reach the corroded bar again and increase the rate of corrosion.

Figure 3 shows the rate of mass loss with time for a corroded bar. It can be noticed that the mass loss increased during passing the current through the bar, and the mass loss rate increased with increasing the rate of current as noticed in the period between 69 and 104 days, and between 202 and 222 days. The current intensity exceeded 200μA/cm^2 , the recommended value by El Maaddawy & Soudki (2003) that was equivalent to 0.07 A, where the length of corroded bar was 700 mm in slab SV. This would cause a significant increase in crack width due to the corrosion.

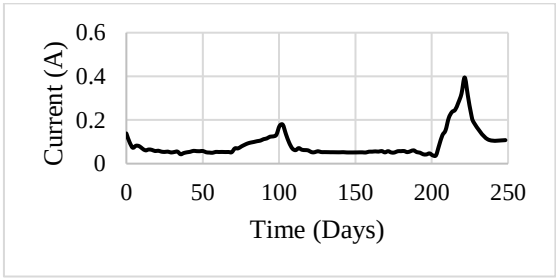

Figure 2: Current time history for SV Slab

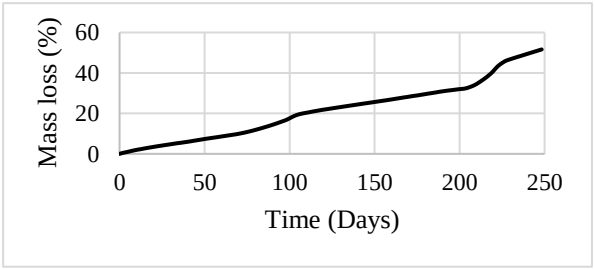

Figure 3: Mass loss rate with time

3.1.2 Half-Cell Potential Measurements

ASTM C876, (2015) considers the high negative reading values of the half-cell potential as an indication of the existence of corrosion. More negative half-cell potential values, higher probability of corrosion. Slab SC used the half-cell potential to estimate the starting time of the occurrence of corrosion to start to calculate the mass loss. After the half-cell read -350 mV, the corrosion time began to be calculated using Faraday's equation. This value was used because based on ASTM C876, (2015) this value indicates that the probability of corrosion occurrence is more than 90%. On the other hand, the half-cell potential was used for the entire test for slab SV to evaluate the corrosion performance. The half-cell readings were recorded once every three days at twenty-four different location that covers the entire corroded area. The reading recorded directly above the flexural reinforcement mesh, twelve readings above the top layer for the flexural mesh and the other twelve readings above the lower ones for the flexural mesh. Figure 4 shows the average half-cell reading versus time. Figure 5 shows the average half-cell reading versus corrosion level. It can

be seen from both figures that the corroded bars in the upper layer had more negative values than the lower one. This result confirms other research result on the corrosion of two-way slabs as Said & Hussein (2019). This could be attributed to the effect of concrete cover, where it was 30 mm for the top layer and 46 mm for the lower layer for the flexural mesh. Hence, the top layer was exposed to more chlorides than the lower one. This result is in good agreement with previous studies that the concrete cover has a significant effect on the half-cell potential values (Klinghoffer, 1995). In both figures, when the corrosion started, there was no variation in the reading of the half-cell. Therefore, half-cell potential test recommended using only as an indication of the corrosion occurrence for un-corroded members.

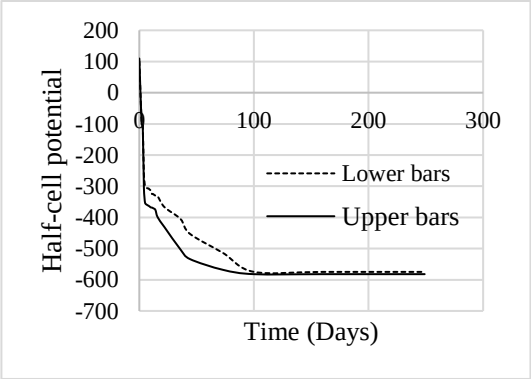

Figure 4: Half-cell potential reading vs. time

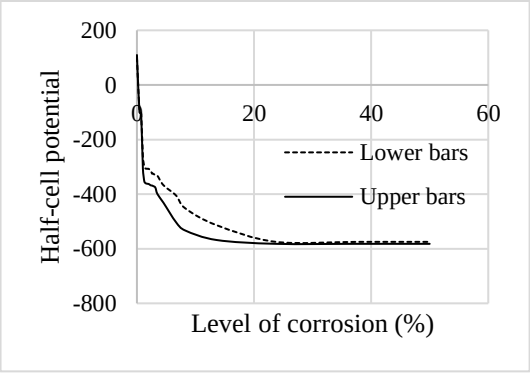

Figure 5: Half-cell potential readings vs. corrosion level

3.2 Test Results after Corrosion

3.2.1 Crack Pattern

Figure 6 shows the crack pattern for both slabs SV and SC. The cracks induced due to the formation of corrosive products beneath the concrete cover, which increases the tensile stress under the cover causing these cracks. The corrosion cracks on slab SC induced directly above the corroded bars, while in slab SV the corrosion cracks did not appear above the corroded bar but were randomly induced above the corroded area. It has been noticed that the crack intensity in slab SV is more than it on slab SC. The crack intensity is defined as the number of cracks over the total number of corroded bars (Said and Hussein, 2019). The cracks were determined by marked them with a blue star on Fig 9. Slab SC has 14 corroded bars that induced 14 longitudinal crack over the corroded area in addition to two inclined other cracks; therefore the crack intensity for SC equals 1.14. Slab SV has 6 corroded bar which induced 17 cracks; therefore, its crack intensity equals 2.83. Thus, it was concluded that constant current gives more realistic crack pattern than constant voltage technique, where the cracks due to corrosion always created parallel to the corroded bars. This result confirms the result of Said & Hussein (2019).

3.2.2 Mass Loss

At the end of the corrosion test, the corroded bars were extracted from the slabs using demolition hammer. The corroded bars were cleaned from the corrosive products following ASTM Standards G1-03 method (ASTM G1, 2003). Then the cleaned bars were weighted to calculate the actual mass loss using the following equation:

$$\%\,\text{mass loss} = \frac{(\text{initial weight - final weight})}{\text{initial weight}} \qquad 2$$

Both techniques showed a close agreement between the actual mass loss and the theoretical mass loss. All bars had actual mass loss less than the theoretical one. This was reached by several researchers (Auyeung, Balaguru and Chung, 2000; Spainhour and Wootton, 2008). This mean that some other process rather than the ionization of iron could have taken place. A kind of this process could be the decomposing that happens to the water due to passing the current through it. The current causing oxidation-reduction reactions which releases oxygen ions as a results of this reaction. During the acceleration process, bubbles were observed during the acceleration process and the previous reason could explain that bubbles (Chen and Luckham, 1994). Therefore, some current has no contribution in causing actual mass loss but it consider in the Faraday's equation that calculate the theoretical mass loss. However, the Faraday's equation gives a close agreement between actual and predicted mass loss regardless to the accelerated corrosion technique used.

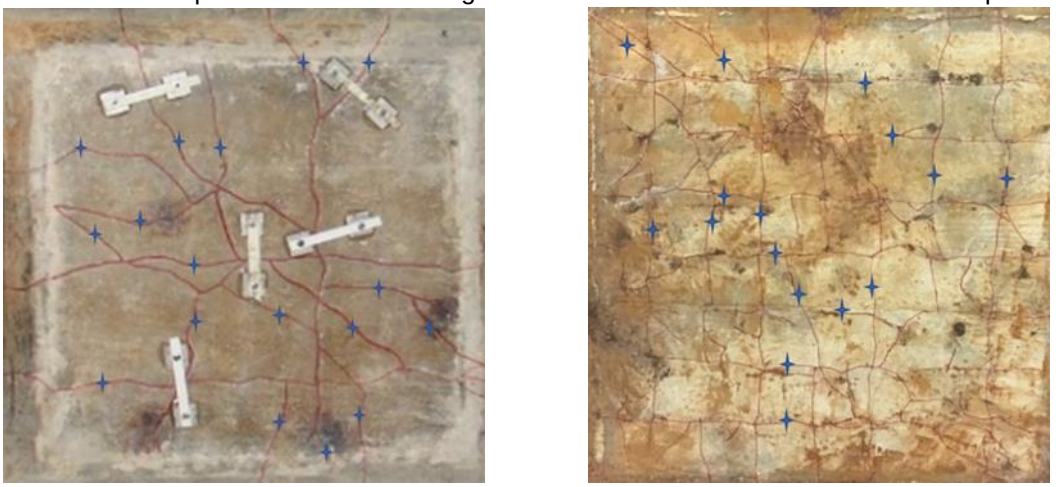

SV SC

Figure 6: crack pattern for the corroded slabs

4 CONCLUSIONS

In this study, a comparison between different laboratory setup to induce corrosion in two-way slabs was presented. Two techniques, constant current and constant voltage were studied. The authors concluded that constant current is more feasible than constant voltage according to the following:

- The most available data acquisition system in most structural labs read voltage, while in constant voltage technique the current is needed to be recorded not the voltage. Thus, there are two options to use constant voltage technique. First to buy data acquisition system read current with enough channel to record the data or follow the technique used in this paper. Both options are expensive. While in constant current technique, each corroded bar needs a power supply.
- The crack pattern in constant current was more realistic than that on constant voltage, where the cracks induced parallel to the corroded bars in constant current.
- The raw data from the constant voltage technique is huge, which need significant effort to collect and process them every day to calculate the theoretical mass loss and to avoid any corruption of the file due to the accumulated recorded data.
- The corrosion time needed to reach the target corrosion level can be readily determined in the constant current technique. While in constant voltage it could not be determined because the current value changes every moment during the test.
- For constant current technique, the current rate is constant in which keep the corrosion rate constant. While in constant voltage technique, the current could reach high values which could exceed the recommended value $200 \mu A/cm^2$ according to El Maaddawy & Soudki (2003). This increase could cause an increase in the concrete crack width leading to more damage than that caused by real corrosion.

5 References

ACI 318-14 (2014) *Building code requirement for structural concrete (ACI 318M-14) and commentary (ACI 318RM-14)*, *Building Code Requirements for Structural Concrete*.

Ahwazi, B. B. N. (2001) *A comparative study of deterioration of bond due to corrosion in different concretes*. McGill University.

Al-Swaidani, A. M. and Aliyan, S. D. (2015) 'Effect of adding scoria as cement replacement on durability-related properties', *International Journal of Concrete Structures and Materials*. Korea Concrete Institute, 9(2), pp. 241–254. doi: 10.1007/s40069-015-0101-z.

Almusallam, A., Al-Gahtani, A. S., Aziz, A. R. and Rasheeduzzafar, A. (1996) 'Effects of reinforcement corrosion on bond strength', *Construction and Building Materials*, 10(2), pp. 123–129.

Altoubat, S., Maalej, M. and Shaikh, F. U. A. (2016) 'Laboratory simulation of corrosion damage in reinforced concrete', *International Journal of Concrete Structures and Materials*. Korea Concrete Institute, 10(3), pp. 383–391. doi: 10.1007/s40069-016-0138-7.

Amleh, L. (2000) *Bond deterioration of reinforcing steel in concrete due to corrosion*. McGill University.

ASTM C876 (2015) 'Standard test method for corrosion potentials of uncoated reinforcing steel in concrete', p. 8. doi: 10.1520/C0876-09.2.

ASTM G1 (2003) *Standard practice for preparing, cleaning, and evaluation corrosion test specimens*.

Auyeung, Y., Balaguru, P. and Chung, L. (2000) 'Bond behavior of corroded reinforcement bars', *Materials Journal*, 97(2), pp. 214–220.

Bonacci, J., Thomas, M., Hearn, N., Lee, C. and Maalej, M. (1998) 'Laboratory simulation of corrosion in reinforced concrete and repair with CFRP wraps', in *Annual Conference of the Canadian Society of Civil Engineering*, pp. 653–662.

Chen, T. Y. and Luckham, P. F. (1994) 'A study of the electrical current passing through water-activated electro-rheological fluids', *Jpournal pf Physics D: Applied Physics*, 27(7), p. 1556.

Cornet, I., Ishikawa, T. and Bresler, B. (1968) 'Mechanism of steel corrosion in concrete structures', *Materials Protection*, 7(3), p. 45.

Davis, J. (2000) *Corrosion: understanding the basics*. doi: 10.1361/cutb2000p001.

Deb, S. and Pradhan, B. (2013) 'A study on corrosion performance of steel in concrete under accelerated condition', in *Proceedings of the International Conference on Structural Engineering Construction and Management, Kandy, Sri Lanka*. Available at: http://dl.lib.mrt.ac.lk/handle/123/9365.

El-Maaddawy, T. and Soudki, K. (2003) 'Effectiveness of impressed current technique to simulate corrosion of steel reinforcement in concrete', *Journal of Materials in Civil Engineering*. American Society of Civil Engineers, 15(1), pp. 41–47. doi: 10.1061/(ASCE)0899-1561(2003)15:1(41).

El-Maaddawy, T., Soudki, K. and Topper, T. (2005) 'Analytical model to predict nonlinear flexural behavior of corroded reinforced concrete beams', *ACI Structural Journal*, 102(4), pp. 550–559.

Kashani, M. M., Crewe, A. J. and Alexander, N. A. (2013) 'Nonlinear stress-strain behaviour of corrosion-damaged reinforcing bars including inelastic buckling', *Engineering Structures*, 48, pp. 417–429. doi: 10.1016/j.engstruct.2012.09.034.

Klinghoffer, O. (1995) 'In situ monitoring of reinforcement corrosion by means of electrochemical methods', *Nordic Concrete Research*, 95(1), pp. 1–13. Available at: http://www.germann.org/Publications/GalvaPulse/2. Klinghofer, O., In Situ Monitoring of Reinforcement Corrosion by means of Electrochemical Methods, Nordic Concrete Research 95

1.pdf.

Kumar, M. K., Rao, P. S., Swamy, B. L. P. and Chandra Mouli, C. (2012) 'Corrosion resistance performance of fly ash blended cement concrete', *Internatioanl Journal of Research in Engineering and Technologi*, 1(3), pp. 448–454. doi: 10.1016/0140-6701(95)93047-7.

Lachemi, M., Al-Bayati, N., Sahmaran, M. and Anil, O. (2014) 'The effect of corrosion on shear behavior of reinforced self-consolidating concrete beams', *Engineering Structures*. Elsevier Ltd, 79, pp. 1–12. doi: 10.1016/j.engstruct.2014.07.044.

Lee, C., Bonacci, J. F., Thomas, M. D. a., Maalej, M., Khajehpour, S., Hearn, N., Pantazopoulou, S. and Sheikh, S. (2000) 'Accelerated corrosion and repair of reinforced concrete columns using carbon fibre reinforced polymer sheets', *Canadian Journal of Civil Engineering*, 27(5), pp. 941–948. doi: 10.1139/cjce-27-5-941.

Pellegrini-Cervantes, M. J., Almeraya-Calderon, F., Borunda-Terrazas, A., Bautista-Margulis, R. G., Chacón-Nava, J. G., Fajardo-San-Miguel, G., Almaral-Sanchez, J. L., Barrios-Durstewitz, C. P. and Martinez-Villafañe, A. (2013) 'Corrosion resistance, porosity and strength of blended portland cement mortar containing rice husk ash and nano-SiO2', *International Journal of Electrochemical Science*, 8(8), pp. 10697–10710.

Pritzl, M. D., Tabatabai, H. and Ghorbanpoor, A. (2014) 'Laboratory evaluation of select methods of corrosion prevention in reinforced concrete bridges', *International Journal of Concrete Structures and Materials*, 8(3), pp. 201–212. doi: 10.1007/s40069-014-0074-3.

Said, M. E. and Hussein, A. A. (2019) 'Induced corrosion techniques for two-way slabs', *Journal of performance of constructed Facility*, 33(3). doi: 10.1061/(ASCE)CF.1943-5509.0001299.

Spainhour, L. K. and Wootton, I. A. (2008) 'Corrosion process and abatement in reinforced concrete wrapped by fiber reinforced polymer', *Cement and Concrete Composites*. Elsevier, 30(6), pp. 535–543.

Talakokula, V., Bhalla, S. and Gupta, A. (2014) 'Corrosion assessment of reinforced concrete structures based on equivalent structural parameters using electro-mechanical impedance technique', *Journal of Intelligent Material Systems and Structures*, 0(0), pp. 1–16. doi: 10.1177/1045389X13498317.

Toongoenthong, K. and Maekawa, K. (2004) 'Interaction of pre-induced damages along main reinforcement and diagonal shear in RC members', *Journal of Advanced Concrete Technology*, 2(3), pp. 431–443. doi: 10.3151/jact.2.431.

Xia, J., Jin, W.-L. and Li, L.-Y. (2012) 'Effect of chloride-induced reinforcing steel corrosion on the flexural strength of reinforced concrete beams', *Magazine of Concrete Research*. Thomas Telford, 64(6), pp. 471–485.

Yoon, S., Wang, K., Weiss, W. and Shah, S. (2001) 'Interaction of reinforced between loading, corrosion, and serviceability of reinforced concrete', *ACI Materials Journal*, 97(6), pp. 637–644.